

# Cations Mediate B-DNA Conformational Heterogeneity<sup>†</sup>

Chad C. Sines, Lori McFail-Isom, Shelley B. Howerton, Don VanDerveer, and Loren Dean Williams\*

Contribution from the School of Chemistry and Biochemistry, Georgia Institute of Technology, Atlanta, Georgia 30332-0400

Received June 22, 2000

**Abstract:** We demonstrate that DNA conformation is sensitive to cationic environment. We describe a high resolution (1.2 Å) potassium form of CGCGAATTCGCG, determined from crystals grown in the presence of spermine and magnesium, along with potassium. The structure was refined with anisotropic displacement-factors by SHELX-97 to an *R*-factor of 13.9%. A comparison of this structure with others, reveals that the conformation of CGCGAATTCGCG varies in direct response to cation type and position. The DNA conformation in the presence of excess magnesium differs from the conformation in the presence of excess spermine. Divalent cations near the minor groove sequester into the lip, which is the region between opposing phosphate groups. Minor groove width is sensitive to, and can be predicted by, cation positions. It appears that minor groove narrowing is facilitated by interactions of cations with opposing phosphate groups.

## Introduction

We have proposed that the locations of mobile inorganic cations and polyamines can be influenced by DNA functional groups.<sup>1,2</sup> These proposed perturbations of the cation “atmosphere” are a modification of previous solution models in which duplex DNA is treated as a featureless cylinder.<sup>3</sup> If delocalized cation atmospheres are perturbed by DNA functional groups, then sequence-specific peaks and troughs of cation concentration might cause conformational heterogeneity. Sequence-specific conformational heterogeneity would then be modulated by the type of cation. Knowing the locations of cations in DNA crystals could allow one to determine the utility of these causative models of DNA conformational heterogeneity. Cation substitution and high-resolution X-ray diffraction experiments ultimately may allow one to characterize solvent regions with sufficient accuracy for construction of “cation maps”.

Here we determine some of the rules governing preferential cation locations around B-DNA and observe certain relationships between the conformation of DNA and the surrounding cationic environment. We describe a high-resolution (1.2 Å) potassium form of CGCGAATTCGCG, determined from crystals grown in the presence of spermine and magnesium, along with potassium. Our initial hypothesis was that at sufficiently high resolution, repeated structure determinations of a given crystal form (space group  $P2_12_12_1$ , unit cell 25, 40, 65 Å) of a fixed DNA sequence would converge. High-resolution data was expected to reveal a “true” DNA conformation and “true” cation types and positions.<sup>4</sup> That hypothesis is shown here to be incorrect. A comparison of high-resolution structures reveals

that the conformation of CGCGAATTCGCG is variable, as are the positions and types of cations. The DNA conformation appears to vary in direct response to the types and positions of cations. Helical parameters such as groove width, base pair roll, helical twist, and propeller twist appear to be sensitive to positions of cations. Minor groove narrowing is modulated by specific localization of cations.

## Materials and Methods

**Crystallization of CGCGAATTCGCG.** Here we describe the crystallization, data collection and reduction, and refinement of a 1.2 Å resolution CGCGAATTCGCG structure obtained from a crystal grown in the presence of potassium along with spermine and magnesium. We have previously described a 1.4 Å resolution CGCGAATTCGCG structure (NDB entry BDL084)<sup>4</sup> obtained from a crystal grown in the presence of sodium, spermine, and magnesium. We have also described a 1.75 Å resolution CGCGAATTCGCG structure (NDB entry BD0005)<sup>5</sup> obtained from a crystal grown in the presence of potassium, spermine, and magnesium, and a 1.8 Å resolution CGCGAATTCGCG structure (NDB entry BD0029)<sup>6</sup> obtained from a crystal grown in the presence of cesium, spermine, and magnesium.

For the high-resolution spermine/potassium structure described here, the ammonium salt of reverse-phase HPLC-purified d(CGCGAATTCGCG) was purchased from the Midland Certified Reagent Company (Midland, TX). Crystals were grown at 22 °C from sitting drops that initially contained 1.0 mM d(CGCGAATTCGCG), 19 mM potassium cacodylate (pH 6.5), 10 mM magnesium chloride, 8.9 mM spermine tetrahydrochloride, and 4.8% 2-methyl-2,4-pentanediol (MPD). The droplets were equilibrated by vapor diffusion against a reservoir of 50% MPD. These crystallization conditions are similar to those of the previous 1.75 Å resolution spermine/potassium structure of CGCGAATTCGCG. Orthorhombic ( $P2_12_12_1$ ) crystals appeared within several days. The crystal chosen for data collection was  $1.1 \times 0.4 \times 0.4$  mm<sup>3</sup>.

**Data Collection and Reduction, and Structure Refinement.** Intensity data were collected on beamline X26C at the National Synchrotron Light Source, Brookhaven National Laboratory. Crystals

\* Address correspondence to this author. E-mail: loren.williams@chemistry.gatech.edu.

<sup>†</sup> Atomic coordinates and structure factors have been deposited in the Nucleic Acid Database (NDB entry BD0041).

(1) McFail-Isom, L.; Sines, C.; Williams, L. D. *Curr. Opin. Struct. Biol.* **1999**, *9*, 298–304.

(2) Williams, L. D.; Maher, L. J. *Annu. Rev. Biophys. Biomol. Struct.* **2000**, *29*, 497–521.

(3) Anderson, C. F.; Record, M. T., Jr. *Annu. Rev. Phys. Chem.* **1995**, *46*, 657–700.

(4) Shui, X.; McFail-Isom, L.; Hu, G. G.; Williams, L. D. *Biochemistry* **1998**, *37*, 8341–8355.

(5) Shui, X.; Sines, C.; McFail-Isom, L.; VanDerveer, D.; Williams, L. D. *Biochemistry* **1998**, *37*, 16877–16887.

(6) Woods, K.; McFail-Isom, L.; Sines, C. C.; Howerton, S. B.; Stephens, R. K.; Williams, L. D. *J. Am. Chem. Soc.* **2000**, *122*, 1546–1547.

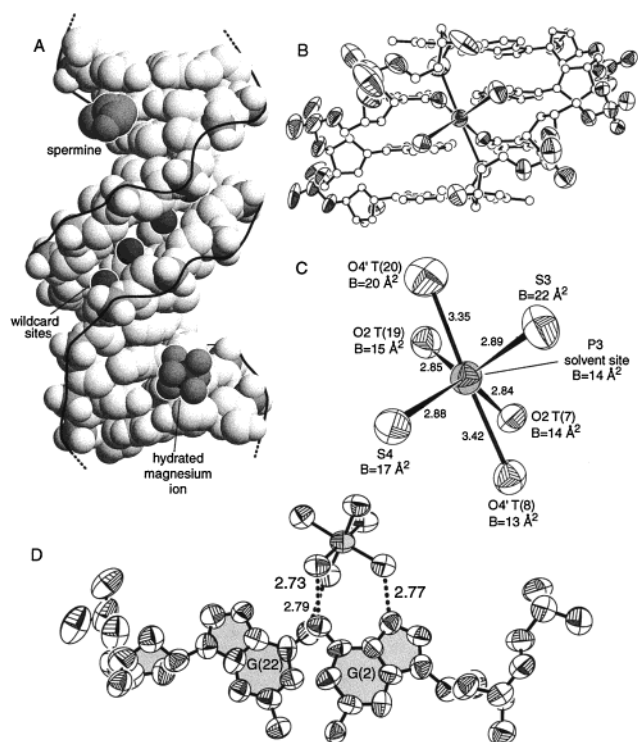


**Figure 1.** Interactions of cations with B-DNA in the 1.2 Å spermine/potassium structure. (A) Space-filling representation of CGCGAATTCGCG and the surrounding cations in the spermine form. A partial spermine molecule is observed on the floor of the major groove of one G-tract. A hydrated magnesium ion is located on the floor of the major groove of the other G-tract. Solvent sites with variable monovalent cation occupancy (wildcard sites) are indicated by dark lone spheres located within the minor groove of the A-tract. The phosphate backbone is highlighted by a solid line that bisects the O1–P–O2 bonds. (B) View into the minor groove of the 5' ApT 3' step of CGCGAATTCGCG, illustrating the four oxygen atoms from the DNA plus two oxygen atoms from water molecules that coordinate one of the wildcard sites. This wildcard site (shaded) is the “P3 solvent site” at the 5' ApT 3' step, as defined previously.<sup>5</sup> Displacement ellipsoids (30% probability) are shown only for the phosphate groups, the P3 solvent site, and its six oxygen ligands. (C) Expanded view illustrating the interactions of the P3 solvent site. S3 and S4 indicate solvent molecules in the secondary hydration layer. (D) View showing the interactions of the major groove magnesium ion and first hydration shell water molecules (residue 25). The hydrated magnesium ion interacts with two guanines that are on opposite strands, offset by one base pair.

were flash frozen by immersion in a stream of 175 K nitrogen gas (Oxford Cryosystems). Intensities were recorded on a Quantum 4 CCD detector at a wavelength of 1.1 Å. Data were processed with the software package HKL.<sup>7</sup> Data collection and reduction statistics and the refinement method and statistics are described in detail in Supporting Information. The quality of the final model, which was refined against 19 368 unique reflections with SHELX-97,<sup>8</sup> is high as inferred from electron density maps [Figure 1 (Supporting Information)], displacement ellipsoids (Figure 1), *R*-factor (13.9%), *R*-Free (21.5%).

## Results

The X-ray structure of native CGCGAATTCGCG was refined against 1.2 Å resolution data. The structure, determined from crystals grown in the presence of potassium, spermine, and magnesium, contains a partial spermine molecule (Figure 1A), one magnesium ion (Figures 1A and 1D), and a fused hexagon

solvent motif within the A-tract minor groove [Figure 1B (Supporting Information)]. We first observed this ion set and hydration motif at 1.4 Å resolution.<sup>4,5</sup> The hexagonal hydration motif has been confirmed by other high-resolution structures of CGCGAATTCGCG,<sup>9</sup> and by the ultrahigh resolution (0.89 Å) Soler-Lopez structure of GCGAATTCG (NDB entry BD0016).<sup>10</sup>

It has been proposed that a 5' ApT 3' step and additional sites within the A-tract minor groove compose favorable locations for monovalent cations.<sup>1</sup> For example, the six-coordinate geometry is suggestive; a 5' ApT 3' step contributes four oxygen ligands to the P3 solvent site (as defined previously<sup>5</sup>), which are complemented by two oxygen ligands from water molecules in the S3 and S4 solvent sites (Figures 1B and 1C).

The 1.2 Å resolution data described here do not definitively resolve whether potassium ions occupy the minor groove of the A-tract. The coordination geometry is consistent with either water or potassium. A series of refined models in which potassium occupancy at the P3 solvent site varies from 0 to 50% (with water occupancy plus potassium occupancy = 100%) give nearly identical *R*-factor, *R*-free, and goodness of fit. When the potassium occupancy increases, the displacement-factor increases moderately without changing the statistical fit of model to data. However the electron density maps are most consistent with moderate potassium occupancy. A model with 100% water at the P3 solvent site shows moderate positive difference intensity ( $2\sigma$ ) at that location, indicating insufficient scattering by the model. A model with 50% water/50% potassium at the P3 solvent site shows moderate negative difference intensity ( $2\sigma$ ), indicating excess scattering. An intermediate model, with 70% water/30% potassium at the P3 solvent site, does not show either positive or negative difference intensity at that location. In sum, the maps suggest partial occupancy by water and potassium, although neither the data nor the geometry provide definitive discrimination. This ambiguity is applicable to many of the “hydration” sites. The final model described here lacks monovalent cations, an omission that is based on convention and should be considered arbitrary.

We have attempted to understand the conformation and ion localization of this new structure in part by a comparison with other high resolution B-DNA structures. The comparison suggests systematic differences in conformation and cation positions. It appears that divalent cations very commonly occupy a region near the top of the minor groove, indicating the utility of a specific geometric definition of this ion-binding region.

**Divalent Cations Selectively Partition into the Lip of the Minor Groove.** The minor groove lip is defined here as a region (i) sufficiently close to a phosphate group for substantial electrostatic interaction, and (ii) on the minor groove side of the phosphate. Specifically, an ion is said to be within the minor groove lip if distance from cation to either phosphate oxygen ( $d_{O^*P-X}$ , where  $*$  = 1 or 2) is less than 5 Å, and if the cation is closer to the O1P than the O2P (i.e.,  $d_{O1P-X} < d_{O2P-X}$ ; in B-DNA, P–O1P bonds are directed roughly across the minor groove). The minor groove lip includes a region above the minor groove and extends down into the minor groove (Figure 2). The conclusions reached here are insensitive to moderate changes in the 5 Å distance cutoff (not shown).

To determine whether divalent cations distribute selectively within the lip of the minor groove, a subset of B-DNA crystal

(7) Otwinowski, Z.; Minor, W. In *Methods in Enzymology, Macromolecular Crystallography*; Carter, J., C. W., Sweet, R. M., Eds.; Academic Press: New York, 1997; pp 276, Part A, pp 307–326.

(8) Sheldrick, G. M. *SHELX-97*; Gottingen University: Germany, 1997.

(9) Tereshko, V.; Minasov, G.; Egli, M. *J. Am. Chem. Soc.* **1999**, *121*, 3590–3595.

(10) Soler-Lopez, M.; Malinina, L.; Liu, J.; Huynh-Dinh, T.; Subirana, J. A. *J. Biol. Chem.* **1999**, *274*, 23683–23686.

**Table 1.** High Resolution B-DNA Structures Containing Divalent Cations

NDB entry	DNA sequence	res. (Å)	divalent cation	divalent cations observed	ions in contact with phosphate group
BD0023 <sup>22</sup>	CCAGTACTGG	0.74	Ca	4	4
BD0014 <sup>39</sup>	CGCGAATTCGCG	1.45	Ca	4	2
BD0007 <sup>13</sup>	CGCGAATTCGCG <sup>a</sup>	1.1	Mg	5	3
BD0012 <sup>9</sup>	CGCGAATTCGCG <sup>a</sup>	1.2	Mg	3	3
BDL084 <sup>4</sup>	CGCGAATTCGCG	1.4	Mg	1	1
BDJ019 <sup>40</sup>	CCAACGTTGG	1.4	Mg	4	2
BD0008 <sup>14</sup>	CGCGAATTCGCG <sup>b</sup>	1.43	Mg	3	3
BD0013 <sup>9</sup>	CGCGAATTCGCG <sup>a</sup>	1.5	Mg	2	2
BDJ025 <sup>41</sup>	CGATCGATCG	1.5	Mg	2	1
BDJ031 <sup>42</sup>	CGATTAATCG	1.5	Mg	1	1

<sup>a</sup> Contains 2'-deoxy-2'-fluoro-arabino-furanosyl thymines. <sup>b</sup> Contains interstrand dithiobis(propane)-cross-links.

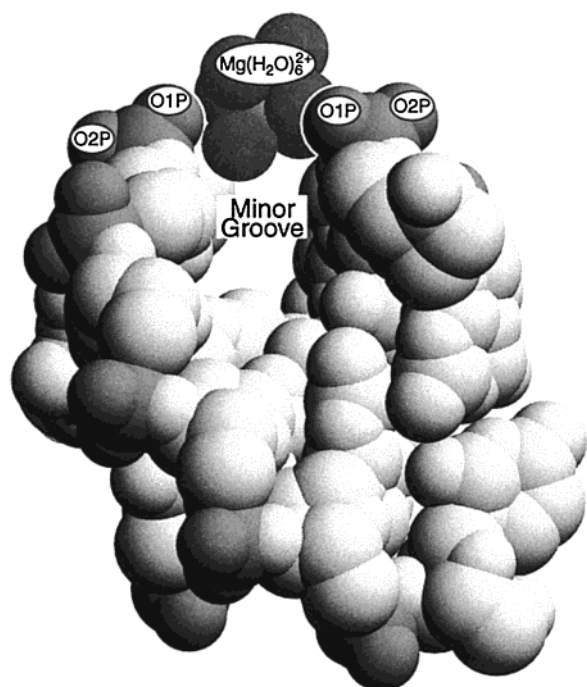


**Figure 2.** A hydrated magnesium ion bound within the lip of the minor groove. First shell water molecules of the magnesium ion are closer to O1P atoms than to O2P atoms. This magnesium ion (no. 38 from NDB entry BD0007,<sup>13</sup> a magnesium form structure) facilitates close approach of O1P of A(18) [ $d_{\text{O1P}-\text{Mg}^{2+}} = 4.1 \text{ \AA}$ ] and O1P of C(11) [ $d_{\text{O1P}-\text{Mg}^{2+}} = 6.1 \text{ \AA}$ ], which are juxtaposed across the minor groove.

structures was selected from the Nucleic Acid Database<sup>11</sup> (NDB) using objective criteria. The structures vary in resolution, space group, DNA length, sequence, and type of divalent cation present. All B-DNA structures with resolution of 1.5 Å or better, and lacking mismatches, flipped-out or unpaired bases, or bound drugs or proteins were selected (11 structures). One structure lacked divalent cations proximal to (within 5.0 Å) any phosphate oxygen and was omitted. The 10 remaining structures, used in this analysis, are listed in Table 1. Two of the selected structures (BD0023, BD0014) contain calcium ions, while the others contain magnesium ions. Calcium and magnesium were treated together here and are indicated by  $\text{X}^{2+}$ . A total of 29 divalent cations ( $\text{X}^{2+}$ ) are contained in the group of selected structures. Six structures are dodecamers with the sequence CGCGAATTCGCG, representing two crystal forms, while four structures are decamers of various sequence and packing arrangements (Table 1). Resolutions range from 0.74 Å (BD0023) to 1.5 Å (BD0013, BDJ025, and BDJ031).

(11) Berman, H. M.; Zardecki, C.; Westbrook, J. *Acta Crystallogr. Sect. D* **1998**, *54*, 1095–1104.

**Table 2.** Contacts between Divalent Cations and Phosphate Groups in B-DNA Crystal Structures<sup>a</sup>

	number of interactions	number with $d(\text{X}^{2+}-\text{O1P}) < d(\text{X}^{2+}-\text{O2P})$
$\text{O}^*\text{P} - \text{X}(\text{H}_2\text{O})_{6,5}^{2+}$	44	32 (73%)
$\text{O}^*\text{P} - \text{X}(\text{H}_2\text{O})_6^{2+}$	36 (81%)	24 (67%)
$\text{O}^*\text{P} - \text{X}(\text{H}_2\text{O})_5^{2+}$	8 (19%)	8 (100%)

<sup>a</sup> Geometric relationships were characterized with the “contact” utility of the program CHAIN,<sup>43</sup> which correctly applies crystallographic symmetry.

The distance  $d_{\text{O}^*\text{P}(i)-\text{X}^{2+(j)}}$  was determined for each phosphate oxygen  $\text{O}^*\text{P}(i)$  (where  $*$  = 1 or 2 and  $i$  = phosphate number) and divalent cation  $\text{X}^{2+(j)}$  ( $\text{X}^{2+}$  = magnesium or calcium and  $j$  = cation number). A fully hydrated  $\text{X}^{2+}$  within contact of a phosphate group is indicated by  $3.5 \text{ \AA} < d_{\text{O}^*\text{P}-\text{X}^{2+}} < 5.0$ . A partially dehydrated  $\text{X}^{2+}$ , with replacement of a first shell water molecule by a phosphate oxygen is indicated by  $d_{[(\text{O}^*\text{P}-\text{X}^{2+})]} < 3.5 \text{ \AA}$ . These distance criteria were empirically determined. A bimodal distribution of contact distances clearly distinguishes between first-shell water mediated and direct modes of  $\text{O}^*\text{P}-\text{X}^{2+}$  interaction. A cluster of  $d_{\text{O}^*\text{P}-\text{X}^{2+}}$  distances centered between 2.0 and 2.5 Å represents direct  $\text{O}^*\text{P}-\text{X}^{2+}$  coordination, with partial dehydration. A cluster centered between 4 and 4.5 Å represents interaction between a phosphate group and fully hydrated  $\text{X}^{2+}$ .

Divalent cations interact preferentially with O1P over O2P in DNA crystal structures. The 10 crystal structures selected contain 44 contacts between phosphate groups and  $\text{X}^{2+}$  (defined by  $d_{\text{O}^*\text{P}-\text{X}^{2+}} < 5 \text{ \AA}$ , Table 2). In 32 instances (73%), the divalent cation is closer to O1P than to O2P and thus is on the minor groove side of the phosphate group. Of the 36 contacts between phosphate groups and fully hydrated  $\text{X}^{2+}$  ions, 24 (67%) are closer to O1P than O2P. Of the eight direct contacts between phosphate oxygen atoms and  $\text{X}^{2+}$  ions, all are with O1P rather than O2P; dehydration occurs specifically at the O1P and never at the O2P in this series of structures. On average, magnesium ions are 0.57 Å closer to O1P atoms than O2P atoms.

A recent B-DNA nonamer structure described by Soler-Lopez et al.<sup>10</sup> (NDB entry BD0016) was screened out of our survey because of unpaired bases (which are inserted into a laterally stacked duplex within the crystal). This structure is of ultrahigh resolution and so merits special discussion here. The final Soler-Lopez model contains five magnesium ions that do not partition preferentially into the lip of the minor groove, with only 40% with  $d_{\text{O}^*\text{P}-\text{Mg}} < 5 \text{ \AA}$  located closer to O1P than O2P. This apparently anomalous distribution of magnesium ions may arise from the location of a chloride ion directly adjacent to the DNA, within the major groove. This chloride ion is likely to perturb the distribution of magnesium ions. Although the distribution of anions around DNA in crystal structures is not well-understood, chloride ions presumably do not reside directly

**Table 3.** Magnesium and Spermine Forms of CGCGAATTCGCG

name	NDB entry	Mg ions <sup>a</sup>	spm atoms <sup>b</sup>	res. (Å)	[spm]/[Mg] (mM) <sup>c</sup>	chemical modification
Magnesium Form						
magnesium/sodium	BD0007 <sup>13</sup>	5	0	1.1	3/25	TAF <sup>d</sup>
magnesium/monovalent-minus	BD0008 <sup>14</sup>	3	0	1.4	0.6/20	X-link <sup>e</sup>
magnesium/Rb_1.2	BD0012 <sup>9</sup>	3	0	1.2	3.2/25	TAF <sup>d</sup>
magnesium/Rb_1.5	BD0013 <sup>9</sup>	2	0	1.5	1.6/6.2	TAF <sup>d</sup>
Spermine Form						
spermine/sodium	BDL084 <sup>4</sup>	1	7	1.4	38/9.6	none
spermine/potassium	here	1	7	1.2	8.9/10	none
spermine/cesium	BD0029 <sup>6</sup>	1	f	1.8	4.5/5.2	none

<sup>a</sup> Number observed in electron density maps. Includes partially occupied ions. <sup>b</sup> A complete spermine molecule is composed of 14 atoms, with a total charge of positive four. <sup>c</sup> Concentrations of spermine and magnesium ions in the initial crystallization solution. <sup>d</sup> 2'-Deoxy-2'-fluoro-arabino-furanosyl thymines. <sup>e</sup> Interstrand dithiobis(propane)-cross-linked. <sup>f</sup> A partial spermine molecule was observed in the electron density maps but was not built into model.

adjacent to the DNA with high frequency, and therefore these magnesium ion locations should be considered anomalous.

**Two Ionic Forms of CGCGAATTCGCG.** A comparison of the high resolution potassium structure of CGCGAATTCGCG described here with other high-resolution structures of the same sequence suggests there are two distinct ionic forms. The two forms differ in conformation and in positions and types of ordered cations (Table 3) but not in DNA crystal packing arrangements (space group  $P2_12_12_1$ , unit cell 25, 40, 65 Å). The intent is to survey structures in a single packing environment. The Liu and Subirana structure of CGCGAATTCGCG that crystallized in space group  $R3$ ,<sup>12</sup> for example, is not considered a member of either class and is not included in our comparison set.

The two classes of CGCGAATTCGCG are called here the spermine form and the magnesium form. The spermine and magnesium forms of CGCGAATTCGCG each exhibit characteristic cations in their electron density maps. The magnesium-form structures contain at least two ordered magnesium ions (from two through five magnesium ions per duplex) but no ordered spermine molecules. Spermine-form structures contain a partially ordered spermine molecule and a single ordered magnesium ion. To describe the various structures here, a nomenclature was developed in which “spermine/sodium structure” indicates a spermine-form structure, obtained from crystals grown with sodium as the primary monovalent cation. Similarly the “magnesium/monovalent-minus structure” indicates a magnesium-form structure, obtained from crystals grown in the absence of monovalent cations.

The observed cation types and locations within this series appear to arise from differences in crystallization conditions (Table 3). The spermine-form structures were crystallized out of solutions with equimolar or excess spermine, ranging from 0.9 to 4.0 [spermine]/[magnesium]. The magnesium-form structures were crystallized out of solutions containing excess magnesium, ranging from 0.03 to 0.26 [spermine]/[magnesium]. Differences in resolution, data quality, or global crystalline order can be ruled out as the origin of differing types and locations of observed cations. For example, only a single magnesium ion is observable in the high-resolution spermine/potassium structure (1.2 Å resolution, Table 3). No additional magnesium ions were detected during painstaking inspection of the finely detailed spermine/potassium electron density maps. Yet two magnesium ions are observable with data limited to 1.5 Å in the magnesium/Rb\_1.5 structure (Table 3).<sup>9</sup> Only a single magnesium ion is observed in structures where a spermine molecule is observed, even when the resolution is significantly better than the

structures lacking observable spermine (i.e., those containing multiple magnesium ions). Conversely a partial spermine molecule is clearly observable in the relatively low-resolution spermine/cesium maps, with data limited to 1.8 Å resolution.<sup>6</sup> Yet, spermine molecules are not apparent in magnesium electron density maps of up to 1.1 Å resolution,<sup>13</sup> indicating that an absence of spermine in this case does not result simply from lower resolution of the data but from different ion localizations within the crystals.

**Ions in the Magnesium Form of CGCGAATTCGCG.** The magnesium form conserves the major groove G-tract magnesium ion (magnesium 25) first observed in the spermine form.<sup>4</sup> From one through four additional magnesium ions (Table 3) also are observable in magnesium structures of the comparison set. These magnesium ions are located primarily within the lip of the minor groove as illustrated in Figure 2. Only one (magnesium 45 in the magnesium/sodium structure) is not fully hydrated by six water molecules. That magnesium ion is coordinated by O1P-(19), the oxygen atom on the minor groove side of phosphate 19, along with five water molecules. In one magnesium structure, monovalent cations are clearly observed within the A-tract minor groove, but apparently only at the 5'ApT3' step.<sup>9</sup> As noted above, spermine molecules have not been observed in magnesium form electron density maps.

**Ions in the Spermine Form of CGCGAATTCGCG.** The spermine form of CGCGAATTCGCG appears to contain three types of cations (Table 3, Figure 1A), clustered in three regions. A partial spermine ion is located in major groove of one G-tract. Seven of the 14 atoms of the spermine molecule are sufficiently ordered for observation. A magnesium ion is located within the major groove of the second G-tract (Figure 1A). This major groove magnesium ion is conserved in all high-resolution structures of CGCGAATTCGCG in our comparison set. The major groove magnesium ion is located within the lip of the minor groove of an adjacent DNA duplex in the crystal. A structure of CGCGAATTCGCG containing cesium as the primary monovalent cation indicates monovalent cations can be distributed within the minor groove of the A-tract of spermine form structures.<sup>6</sup> A structure of CGCGAATTCGCG containing thallium(I) as the primary monovalent cation indicates monovalent cation occupancy primarily within the G-tract major groove (S. B. Howerton and L. D. Williams, unpublished). Thallium and cesium scatter X-rays much more strongly than potassium and are therefore easier to detect by X-ray diffraction.

**Conformational Differences in the Magnesium and Spermine Forms of CGCGAATTCGCG.** The seven high-resolu-

(12) Liu, J.; Malinina, L.; Huynh-Dinh, T.; Subirana, J. A. *FEBS Lett.* **1998**, *438*, 211–4.

(13) Tereshko, V.; Minasov, G.; Egli, M. *J. Am. Chem. Soc.* **1999**, *121*, 470–471.

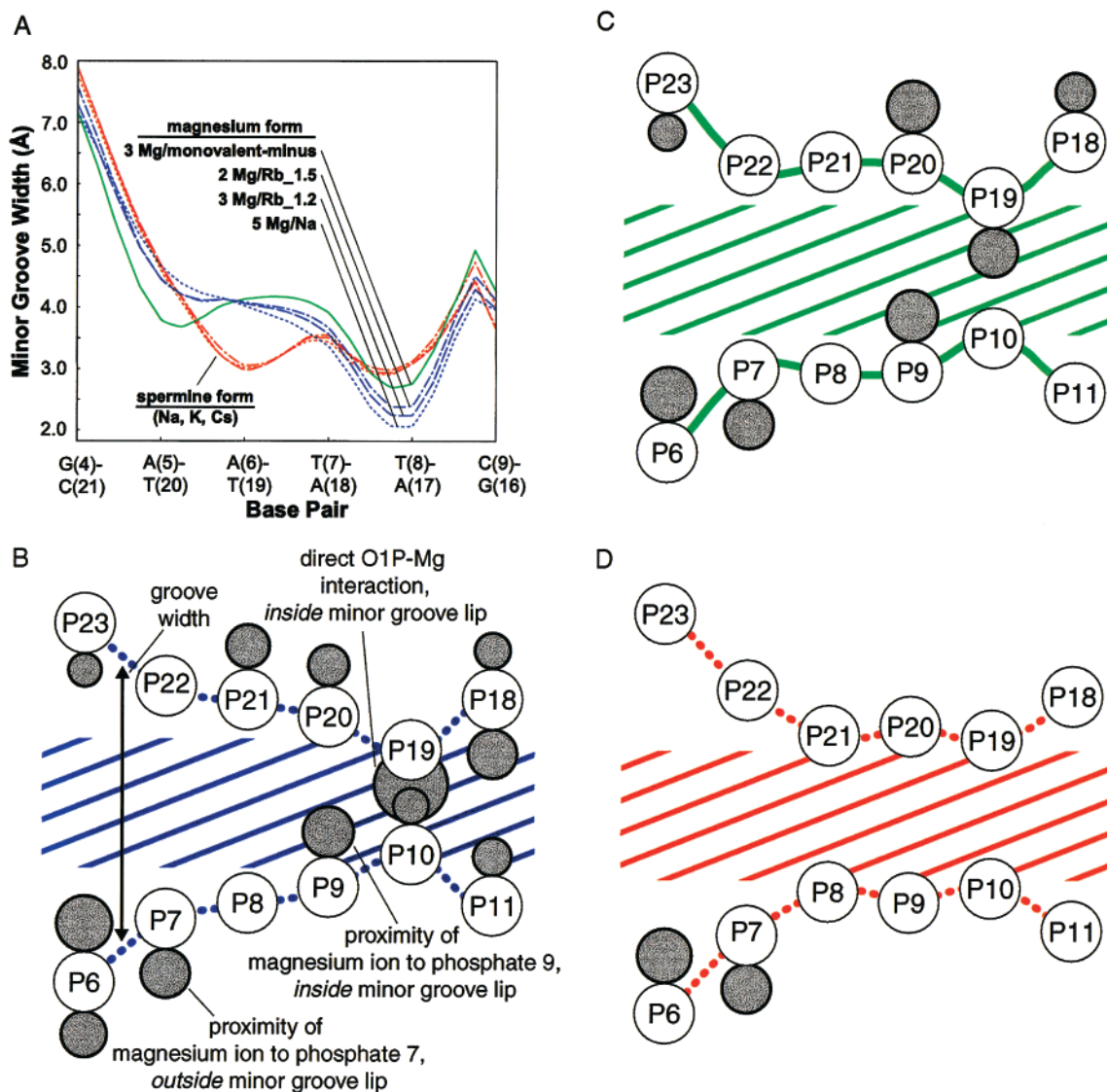


**Figure 3.** Relationship between minor groove width and cation positions in seven high-resolution CGCGAATTCGCG structures. These structures are in the same “crystal form”, so that lattice forces are invariant. Minor groove width profiles were calculated with the program CURVES (version 5.30),<sup>38</sup> which provides a continuous description of groove geometry. The spermine form groove widths are shown in red (dotted line; spermine/sodium, dashed line; spermine/potassium, dot-dashed line; spermine/cesium). The magnesium form groove widths are blue (dotted line; magnesium/sodium, dashed line; magnesium/rubidium\_1.2, dot-dashed line; magnesium/rubidium\_1.5) except the monovalent minus structure, which is solid green. (A) Minor groove width profiles of all seven structures. (B) Groove width and magnesium-phosphate proximities in the magnesium/sodium form of CGCGAATTCGCG. Groove width is indicated quantitatively by vertical displacement. Phosphorus atoms are denoted by circled P’s. Proximities of magnesium ions to phosphorus atoms are indicated quantitatively by gray circles with radii =  $1/d_{\text{Mg-P}}$ ,  $d_{\text{Mg-P}} > 7 \text{ \AA}$  excluded. Magnesium ions located within the minor groove lip are indicated by circles within the minor groove. A magnesium ion is to be within the minor groove lip if  $d_{\text{O1P-Mg}} < d_{\text{O2P-Mg}}$ . (C) Groove width and magnesium-phosphate proximities in the magnesium/monovalent-minus form of CGCGAATTCGCG. (D) Groove width, magnesium-phosphate proximities, and monovalent cation binding sites in the spermine/sodium form of CGCGAATTCGCG.

tion structures of CGCGAATTCGCG are separable into two distinct classes by conformational attributes such as minor groove width profiles (Figure 3). The members of the two conformational classes correspond with the members of the two ionic forms (magnesium and spermine) and thus will be referred to here by that nomenclature. The narrowing of the A-tract minor groove of the magnesium form is more extreme than that of the spermine form. The groove width global minimum is offset by two base pairs in the two forms. In the magnesium form the width of the minor groove reaches a local maximum at A(6)-T(19), just where that of the spermine form reaches a global minimum. The narrowing of the A-tract minor groove of the magnesium form minor groove is variable, while that of the spermine form is conserved.

The two ionic forms of CGCGAATTCGCG also differ in base pair slide and roll and in helical twist (Figure 4). The helical parameters of each class are tightly clustered, with the exception of the magnesium/monovalent minus structure, which is a conformational outlier. Differences are focused in the central part of the dodecamer but extend out to one of the helical termini.

**Relationship between Groove Width and Cation Positions.** The degree of minor groove narrowing of the magnesium form appears to be correlated with concentration of magnesium ions within the minor groove lip. The relationship between groove narrowing and magnesium concentration and position is shown in Figure 3B–D. Groove width is indicated by vertical distance. Proximity of magnesium ion to phosphorus atom is indicated

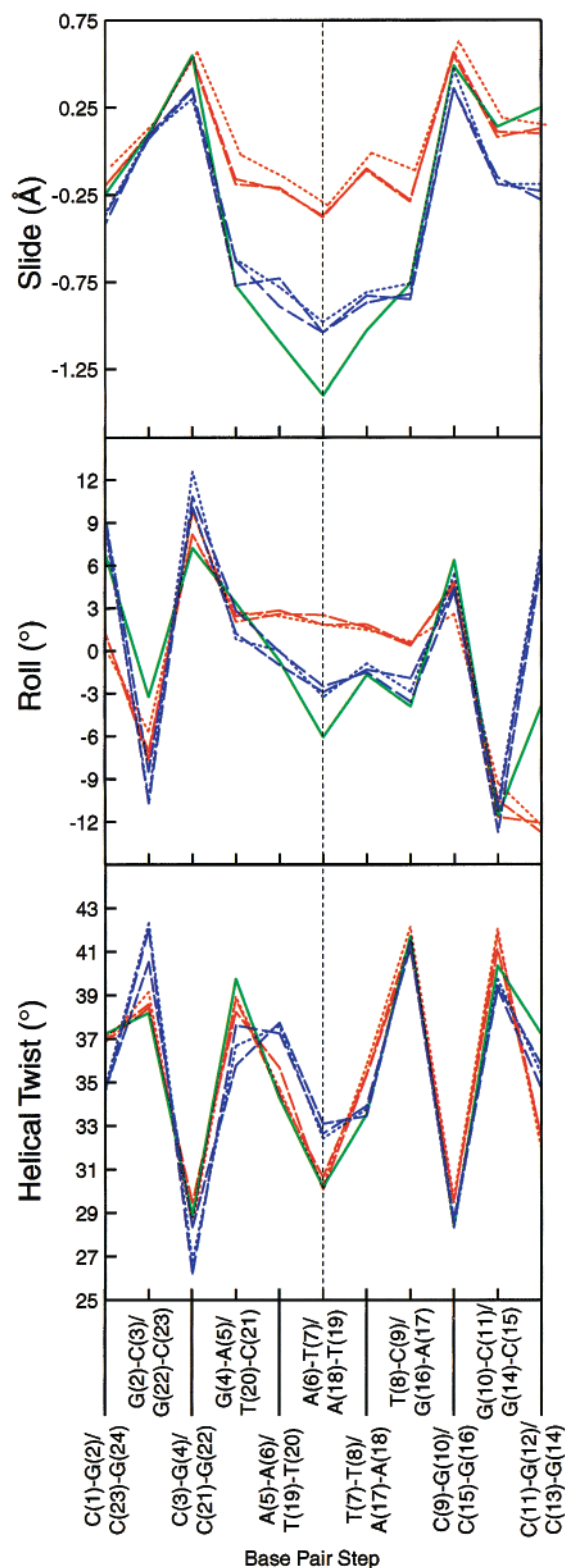


**Figure 4.** Helical parameters are clustered into two distinct families, with the exception of one outlier (the magnesium/monovalent-minus structure). Slide, roll, and helical twist of seven high-resolution structures of CGCGAATTCGCG. The color and coding schemes are the same as in Figure 3.

by circle radius ( $1/d_{\text{Mg-P}}$ ) with  $d_{\text{Mg-P}} > 7 \text{ \AA}$  excluded. Magnesium ions with  $d_{\text{O1P-X}} < d_{\text{O2P-X}}$  are indicated by the circles inside the minor groove (i.e., within the lip of the minor groove). Magnesium ions with  $d_{\text{O1P-X}} > d_{\text{O2P-X}}$  are indicated by the circles outside the minor groove. All magnesium

ions are treated equally, regardless of apparent crystallographic occupancy.

Magnesium–phosphate electrostatic interactions within the minor groove of the magnesium form appear to correlate with narrowing. The magnesium/sodium structure (Table 3) has the highest magnesium concentration within the minor groove lip and the narrowest minor groove (Figure 3B). The global minimum of the minor groove width occurs just where magnesium concentration is the greatest and magnesium–phosphate distances are the shortest. Strong electrostatic interactions between cross-strand phosphate groups and magnesium ions must characterize this region, where phosphate 19 opposes phosphate 10 [i.e., at base pair T(8)-A(17)]. The large circle adjacent to P19 indicates very close proximity to a magnesium ion ( $d_{\text{P-Mg}} = 3.5 \text{ \AA}$ ) and strong electrostatic interaction. In this region of acute minor groove narrowing, several sets of opposing phosphate groups interact with magnesium ions contained within the minor groove lip. This clustered set of electrostatic interactions almost certainly facilitates the extreme narrowing of the minor groove observed in this structure. The groove width increases as phosphate–magnesium electrostatic interactions within the lip decrease. In progressing from P19–P10 to P20–P9 to P21–P8, etc., favorable electrostatic interactions within the lip are increasingly attenuated; the groove width increases. In the region P23–P6 region, magnesium ions are similarly observed within the minor groove lip. However lattice forces prevent minor groove narrowing in this region (an adjacent duplex protrudes into the minor groove).

In the magnesium/monovalent-minus structure, obtained from crystals grown in the absence of monovalent cations,<sup>14</sup> the global minimum in minor groove width similarly occurs at P19–P10, where the magnesium concentration within the lip is greatest. However in this case the observed magnesium concentration within the lip is less than in the magnesium/sodium structure, and the groove width is greater. The spermine structures do not contain magnesium ions in the P19–P10 region and exhibit the widest narrow groove at that point.

The minor groove width profile is highly conserved in the spermine form of CGCGAATTCGCG (Figure 3A). The minor groove profile is invariant to monovalent cation type ( $\text{Na}^+$ ,  $\text{K}^+$ , or  $\text{Cs}^+$ ), refinement protocol (XPLOR with isotropic displacement-factors versus SHELX-97 with anisotropic displacement-factors) and resolution ( $1.8 \text{ \AA}$  versus  $1.2 \text{ \AA}$ ). The width of the minor groove reaches a global minimum near the center of the A-tract [A(6)-T(19)], rises at the next base pair [T(7)-A(18)], and falls to a secondary minimum at base pair T(8)-A(17). The width of the minor groove is more uniform along the A-tract in the spermine form than in the magnesium form. The single divalent cation observed in the electron density maps does not appear to play a role in maintaining the narrowness of the A-tract minor groove (Figure 3D).

The high degree of reproducibility of the spermine form groove profile of CGCGAATTCGCG establishes that error limits are low. In view of this high reproducibility, it seems unlikely that the observed differences between forms and within the magnesium form arise from coordinate error.

**Do Monovalent Cations Contribute to High Propeller Twisting of AT Base Pairs?** A comparison of high-resolution structures of CGCGAATTCGCG suggests interactions of cations can mediate the high propeller twist of AT base pairs. The NDB contains six high-resolution “monovalent-plus” structures of CGCGAATTCGCG (space group  $P2_12_12_1$ , unit

(14) Chiu, T. K.; Kaczor-Grzeskowiak, M.; Dickerson, R. E. *J. Mol. Biol.* **1999**, *292*, 589–608.

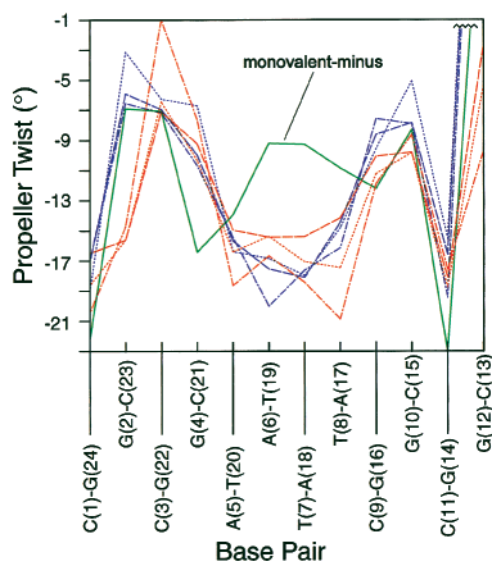


**Figure 5.** Propeller twists of seven high-resolution structures of CGCGAATTCGCG. The coding scheme is the same as in Figure 3.

cell 25, 40, 65 Å; Table 3). These structures were determined from crystals grown in the presence of monovalent cations along with magnesium and spermine. The NDB contains one high-resolution “monovalent-minus” structure of CGCGAATTCGCG with that same crystal packing (Table 3). This structure was determined from a crystal grown in the presence of magnesium and spermine, but in the absence of monovalent cations. These operational definitions, based on crystallization conditions rather than crystal contents, are necessary because none of the structures are electroneutral; the positions and crystalline concentrations of monovalent cations are generally unknown.

For the monovalent-plus structures, the average AT propeller twist is significantly greater in magnitude than the average GC propeller twist. Propeller twist values are shown in Figure 5. Averaged over six high-resolution monovalent-plus structures of CGCGAATTCGCG the propeller twist of AT base pairs is  $-16.7^\circ \pm 0.7^\circ$  (95% confidence limits), while that of GC base pairs is  $-8.5^\circ \pm 3.1$ . This difference in average propeller twists is greater than the sum of the confidence limits and therefore is statistically significant.

In the monovalent-minus structure the average propeller twist is invariant to base pair type. The AT and GC average propeller twists are the same ( $-11^\circ$ ). Further, the average propeller twist of the four AT base pairs in the monovalent-minus structure is less than the average in any of the monovalent-plus structures. The difference in average AT propeller twist of any monovalent-plus structure from that of the monovalent-minus structure is uniformly greater than the confidence limits.

The propeller twists of the two base pairs of the central 5'ApT3' step of CGCGAATTCGCG may be enhanced by interactions with monovalent cations. High negative propeller twist of base pairs A(6)-T(19) and T(7)-A(18) is observed in structures obtained from crystals grown in the presence of sodium,<sup>4,13</sup> potassium (here), rubidium,<sup>9</sup> and cesium<sup>6</sup> (Figure 5). The average propeller twist of these two base pairs in these six monovalent-plus structures is  $-17.2^\circ \pm 0.8$ . A marked attenuation of these propeller twists is observed in the monovalent-minus structure, where the propeller twist is decreased in magnitude to  $-9.2^\circ$  for both base pairs. This attenuation of propeller twist is statistically significant by a variety of measures such as Chauvenet's criterion.<sup>15</sup> Therefore, for base pairs A(6)-T(19) and T(7)-A(18), the propeller twists in the magnesium/

monovalent-minus structure are attenuated to a statistically significant extent relative to those of six structures obtained in the presence of monovalent cations.

An alternative cause of the attenuated propeller twist in the monovalent-minus structure is chemical modification. Some of the dodecamer structures, including the monovalent minus structure, are composed of chemically modified DNA (Table 3). We will assume here, as have others,<sup>14,16</sup> that the effects of those modifications on conformation are negligible. With respect to the magnesium/monovalent-minus structure, Chui et al. observe that “The tether between the two central base-pairs is sufficiently long that it introduces little strain into the helix.” They conclude that “[the] structural effect of a slack tether between closely spaced adenine bases is virtually zero.”<sup>14</sup> However, determinations of monovalent minus structures of unmodified DNA are required to validate this assumption.

## Discussion

In solution, inorganic cations and polyamines are found at high concentration within the first several hydration layers of DNA.<sup>3,17,18</sup> Changes in cation type and concentration can induce large-scale conformational transitions in DNA.<sup>19,20</sup> In crystals, the solvent region immediately surrounding DNA has been characterized as pure water,<sup>21</sup> with only occasional penetration by cations. However as resolution continues to increase, cations are seen in ever higher frequency proximal to crystalline DNA oligonucleotides.<sup>4,6,9,10,22,23</sup>

The ability of DNA functional groups to influence local cation concentration is consistent with NMR experiments,<sup>24,25</sup> molecular dynamics simulations,<sup>17,18,26–28</sup> and X-ray diffraction experiments.<sup>4–6,9,29,30</sup> For example we have previously observed that divalent cations avoid DNA amino groups.<sup>5</sup> Here we show that divalent cations partition within the “lip of the minor groove”, interacting preferentially with O1P over O2P of B-DNA (Figure 2 and Table 2). These interactions are most prevalent when the minor groove is especially narrow. It appears that dehydration of magnesium occurs preferentially at the O1P over the O2P. In sum, cation localization is influenced by DNA sequence and conformation, along with cation charge, size, dehydration energy, etc.

**Structural Roles for Cations?** Chiu and co-workers (1999) recently disagreed with our suggestion that cations influence

(15) Young, H. D. *Statistical Treatment of Experimental Data*; McGraw-Hill: New York, 1962.

(16) Tereshko, V.; Minasov, G.; Egli, M. *J. Am. Chem. Soc.* **1999**, *121*, 6970.

(17) Feig, M.; Pettitt, B. M. *Biophys. J.* **1999**, *77*, 1769–81.

(18) Auffinger, P.; Westhof, E. *J. Mol. Biol.* **2000**, *300*, 1113–1131.

(19) Pohl, F. M.; Jovin, T. M. *J. Mol. Biol.* **1972**, *67*, 375–396.

(20) van de Sande, J. H.; McIntosh, L. P.; Jovin, T. M. *EMBO J.* **1982**, *1*, 777–782.

(21) Drew, H. R.; Dickerson, R. E. *J. Mol. Biol.* **1981**, *151*, 535–556.

(22) Kielkopf, C. L.; Ding, S.; Kuhn, P.; Rees, D. C. *J. Mol. Biol.* **2000**, *296*, 787–801.

(23) Vlieghe, D.; Turkenburg, J. P.; Van Meervelt, L. *Acta Crystallogr. D Biol. Crystallogr.* **1999**, *55*, 1495–502.

(24) Denisov, V. P.; Halle, B. *Proc. Natl. Acad. Sci. U.S.A.* **2000**, *97*, 629–33.

(25) Hud, N. V.; Sklenar, V.; Feigon, J. *J. Mol. Biol.* **1999**, *286*, 651–60.

(26) Young, M. A.; Beveridge, D. L. *J. Mol. Biol.* **1998**, *281*, 675–687.

(27) Young, M. A.; Jayaram, B.; Beveridge, D. L. *J. Am. Chem. Soc.* **1997**, *119*, 59–69.

(28) Hamelberg, D.; McFail-Isom, L.; Williams, L. D.; Wilson, W. D. *J. Am. Chem. Soc.* **2000**, *122*, in press.

(29) Bartenev, V. N.; Golovamov, E. I.; Kapitonova, K. A.; Mokukskii, M. A.; Volkova, L. I.; Skuratovskii, I. Y. *J. Mol. Biol.* **1983**, *169*, 217–234.

(30) Rosenberg, J. M.; Seeman, N. C.; Kim, J. J. P.; Suddath, F. L.; Nicholas, H. B.; Rich, A. *Nature* **1973**, *243*, 150–154.

DNA conformation, and concluded that the conformation of crystalline CGCGAATTCGCG is invariant in the presence or absence of monovalent cations. Specifically they concluded that the conformations of our spermine/sodium structure (structure X) and their magnesium/monovalent-minus structure (structure X-Link) are virtually identical. They believe that the minor groove has the same width in these two structures. We do not agree with their assessment. It seems clear that in many important aspects, including minor groove width, propeller twist, slide, roll, and helical twist, conformations of our spermine/sodium structure and their magnesium/monovalent-minus structure differ (Figures 3–5). The differences are significant upon inspection and when assayed by objective statistical criteria. In fact the conformation of their magnesium/monovalent-minus structure is a statistical outlier from the conformations of other high resolution CGCGAATTCGCG structures in Table 3. The observed differences are consistent with the importance of cations in modulating DNA conformation. However, the effects of the chemical modification of the magnesium/monovalent-minus structure and some of the other structures in the comparison set (Table 3) currently cannot be excluded as a possible origin of some or all of the differences in conformation.

It has been thought that sodium, potassium, magnesium, or calcium ions surrounding B-DNA remain hydrated and mobile and do not engage in specific structural roles. Water molecules in contrast have been thought to be intrinsic structural components of DNA, as in the “spine of hydration”. In our view this prohibition on structural roles for cations but not for water molecules is self-contradictory. The potential energy surface felt by a cation in the vicinity of DNA is more highly featured than that felt by a water molecule. The forces between cations and DNA are greater and fall off with distance more gradually than forces between water molecules and DNA. Can a water molecule be “structural” when a potassium ion cannot?

In our view many of the water molecules determined by nucleic acid crystallography should be considered “structural wildcards”. For many solvent sites the fractional occupancy of water and monovalent cation is variable, changing with crystallization conditions, etc. For example the P3 solvent site, in the minor groove of an 5'ApT3' step, is unambiguously fully occupied by water in the monovalent-minus structure but is a cation/hybrid under other conditions.<sup>6,9</sup> Under many common experimental conditions, cation occupancy can be essentially undetectable. As described here, even atomic resolution data cannot discriminate between full occupancy water molecules and water/potassium hybrids. The statistical fit of model to data is essentially invariant throughout a series of models with varying water and potassium occupancy. The electron density maps suggest potassium occupancy. Historically, assignment of electron density peaks as water molecules has often been based on various assumptions, but not on the diffraction data.

**In the Crystalline State, CGCGAATTCGCG Is Found in Two Distinct Ionic and Conformational Forms.** The comparison here of high-resolution structures of CGCGAATTCGCG reveals two distinct ionic forms; a spermine form and a magnesium form. These two forms differ in crystallization conditions, in positions and types of cations observed in electron density maps, and in DNA conformation (Figures 3–5). The differences do not arise simply from variations in data quality or global crystalline order, although cations in addition to those observed thus far will no doubt be revealed as resolution continues to increase.

The spermine form of CGCGAATTCGCG contains a partially ordered spermine molecule and one magnesium ion per

dodecamer duplex. Both are located on the floor of the G-tract major groove. The magnesium is located in the minor groove lip of an adjacent DNA duplex. The magnesium form conserves the major groove magnesium ion, and contains from one through four additional magnesium ions per duplex. These additional magnesium ions are located predominantly within the lip of the minor groove. The magnesium form lacks spermine.

The two ionic forms of CGCGAATTCGCG characterized here display distinctive profiles of the A-tract minor groove. The magnesium form shows the most acute narrowing and greater variation in groove width both within a given structure and between structures. The location and extent of minor groove narrowing correlates with magnesium localization within the minor groove lip.

The minor groove width profile of the spermine form is more uniform along the A-tract and is highly conserved between structures. The magnesium form groove width reaches a local maximum just where the spermine form reaches a global minimum. The results here support a mechanism in which groove width is modulated by direct shielding of opposing phosphate groups, as when cations localize within the lip.

**Cooperative Displacements of Cations and DNA Phosphate Groups.** The combined data support a model in which motions of DNA and motions of cations are coupled. Young and Beveridge<sup>26</sup> used molecular dynamics simulations to “observe” selective partitioning of monovalent cations into the minor groove of AT-tracts, and suggested this might be the ultimate cause of A-tract groove narrowing. Feig and Pettitt<sup>17</sup> and Hamelberg and co-workers<sup>28</sup> have extended that work to show specific reduction in the width of the minor groove upon entry of sodium. This work suggests similar fluctuational time scales of DNA conformation and of cation positions.

A model in which motions of cations are cooperative with changes in DNA conformation predicts that variation of cation positions would correlate with variation of DNA conformation. The crystallographic experiment averages over an ensemble of cation positions and DNA conformations. Therefore smeared-out cations (unobserved or partially occupied) should be accompanied by high displacement-factors of phosphate groups. Phosphate group positional disorder should be anisotropic, with directionality influenced by the electronic force vectors originating from the various cation positions.

In intermediate- and low-resolution structures, at low temperature where displacement-factors indicate static disorder, the displacement-factors of phosphate groups are indeed greater than for the rest of the DNA.<sup>31</sup> However, this resolution realm provides little information on cation positions or anisotropic positional disorder of phosphate groups.

At atomic resolution, displacement ellipsoids are greater for some phosphate groups than for other parts of the DNA (Figures 1B and 2S). The disorder of phosphate groups is not uniform in direction or magnitude. The direction of the long moment of the ellipsoids is consistent with cation disorder. Although some cations are observable at atomic resolution, positional disorder is generally unresolved, giving unpaired “partial occupants”.

The possibility of direct coupling of cation and phosphate displacements can be addressed by comparing ionic forms of CGCGAATTCGCG. In fact, a model in which displacement of cations is cooperative with variation in conformation is consistent with conformational variation described here among a series of high and atomic-resolution structures. Variation of

(31) Drew, H. R.; Samson, S.; Dickerson, R. E. *Proc. Natl. Acad. Sci. U.S.A.* **1982**, *79*, 4040–4044.



the conformation of CGCGAATTCGCG is associated with variation in cation positions. The minor groove width is minimized when phosphate groups interact most extensively with cations (Figure 3).

At ultrahigh resolution, the observation of paired, alternate calcium and phosphate positions provides strong evidence for coupling. Rees and co-workers assigned paired, partially occupied calcium ions that bind to a DNA decamer in an either/or configuration.<sup>22</sup> Similarly the DNA is disordered. Six of the nine phosphate groups and two of the four calcium ions are statically disordered.

**Do Monovalent Cations Contribute to Propeller Twisting of Base Pairs?** AT base pairs tend to be more highly propeller-twisted than GC base pairs.<sup>32</sup> The greater number of hydrogen bonds is thought to impart a greater torsional rigidity within GC base pairs than in AT base pairs. Although the present set of high resolution structures (Table 3) does not allow us to exclude contributions from chemical modification, the high propeller twist of AT base pairs may be related to interactions with cations. When monovalent cations are rigorously omitted from the crystallization solution of CGCGAATTCGCG,<sup>14</sup> differences in propeller twists of AT and GC base pairs vanish. The locations of monovalent cations in X-ray structures<sup>1,4–6,9,29,30</sup> suggest a simple and direct structural basis for their influence on propeller twist. The monovalent cation binding sites of the primary hydration layer of the A-tract minor groove interleave the base pair planes. When the minor groove is narrow, the positions of the solvent sites are restrained to offset locations by interactions with O4' atoms as shown in Figure 1C. Propeller twist improves the coordination geometry. Therefore, the greater chelation forces of monovalent cations in comparison to water molecules might modulate propeller twist in some cases. This causal model of propeller twist is consistent with observed correlations between the presence of monovalent cations and propeller twist (here), and between propeller twist and groove width.<sup>32</sup>

**Not All Cations Are Observed by X-ray Diffraction.** The spermine and magnesium classification scheme used here arises from cation locations as observed in crystallographic experiments. The spermine and magnesium forms are unambiguously distinguished by differential locations and concentrations of ordered cations and by DNA conformation. The classification scheme is not based on locations of all cations within the crystals of CGCGAATTCGCG. That information is not currently accessible. Even in ultrahigh resolution DNA structures<sup>10,22</sup> negative charges contributed by phosphates are not fully compensated by observed positive charges. Cations in addition to those observed in the electron density maps, as required for charge neutrality, are contained in these DNA crystals.

## Conclusions

Various metal ions specifically stabilize Z-DNA,<sup>19,20</sup> G-quartets,<sup>33,34</sup> and other noncanonical conformations.<sup>35</sup> Recently, it has been demonstrated that divalent zinc, nickel, and cobalt can intercalate in DNA, substituting divalent cations for imino protons, to form "M-DNA".<sup>36</sup> The variation of DNA conforma-

tion with changing cation positions, while sequence and lattice are fixed, demonstrated here indicates that specific interactions between DNA and surrounding cations contribute to conformational heterogeneity of B-form CGCGAATTCGCG. The possibility of observing additional ionic forms in additional conformational states is high. The two forms described here appear to be discrete and exclusive in that either spermine plus one magnesium ion or multiple magnesium ions are observed.

We anticipate that in crystals, the effects of ions on DNA conformation variation would be attenuated in comparison to those in the solution state. In the crystalline environment (i) intermolecular electrostatic forces would compete with intramolecular forces, (ii) sequence-specific effects on cation distributions would be perturbed by lattice effects, and (iii) steric lattice restraints would dampen the structural consequences of electrostatic forces. These considerations support the proposal by Crothers that the A-tract conformation of CGCGAATTCGCG might be different in crystals and dilute solution.<sup>37</sup> If electrostatic forces are significant, deviations of solution from crystalline behavior should be least pronounced for short-range phenomena such as groove width variation, and most pronounced for long-range phenomena such as DNA bending. In fact the cation-related perturbations observed here, and by Rees and co-workers,<sup>22</sup> are most pronounced for local phenomenon. Solution-like A-tract bending has not been observed thus far in oligonucleotide crystals.

A combination of technical advances should allow us to significantly increase the detail of the "cation map" surrounding DNA. The quality of crystals grown in a host of laboratories continues to increase. The quality and availability of synchrotron radiation sources and fast readout detectors continues to increase. Full matrix refinement with application of anisotropic displacement-factors is now routinely applicable to large molecules, if data quality is sufficient. Substitution of potassium with thallium may allow construction of complete "monovalent cation maps" surrounding DNA and RNA.

**Acknowledgment.** This work was supported by the National Science Foundation (Grant MCB-9976498) and the American Cancer Society (Grant RPG-95-116-03-GMC). This research was carried out in part at the National Synchrotron Light Source, Brookhaven National Laboratory, which is supported by the U.S. Department of Energy, Division of Materials Sciences and Division of Chemical Sciences under contract number DE-AC02-98CH10886. We thank Drs. Dieter Schnieder, George Sheldrick, Jonathan Chaires, W. David Wilson, Donald Hamelberg, and David Draper for helpful discussions.

**Supporting Information Available:** Tables, figures and a description of crystal data, structure solution and refinement (PDF). This material is available free of charge via the Internet at <http://pubs.acs.org>.

JA002244P

(37) Haran, T. E.; Kahn, J. D.; Crothers, D. M. *J. Mol. Biol.* **1994**, *244*, 135–143.

(38) Stofor, E.; Lavery, R. *Biopolymers* **1994**, *34*, 337–346.

(39) Liu, J.; Subirana, J. A. *J. Biol. Chem.* **1999**, *274*, 24749–52.

(40) Prive, G. G.; Yanagi, K.; Dickerson, R. E. *J. Mol. Biol.* **1991**, *217*, 201–214.

(41) Grzeskowiak, K.; Yanagi, K.; Prive, G. G.; Dickerson, R. E. *J. Biol. Chem.* **1991**, *266*, 8861–8883.

(42) Quintana, J. R.; Grzeskowiak, K.; Yanagi, K.; Dickerson, R. E. *J. Mol. Biol.* **1992**, *225*, 379–395.

(43) Sack, J. *Chain: A Crystallographic Modelling Program*; Baylor College of Medicine: Waco, TX, 1990.

(32) Berman, H. M. *Biopolymers* **1997**, *44*, 23–44.

(33) Williamson, J. R.; Raghuraman, M. K.; Cech, T. R. *Cell* **1989**, *59*, 871–880.

(34) Smirnov, I.; Shafer, R. H. *J. Mol. Biol.* **2000**, *296*, 1–5.

(35) Wohlrab, F.; Wells, R. D. *J. Biol. Chem.* **1989**, *264*, 8207–13.

(36) Aich, P.; Labiuk, S. L.; Tari, L. W.; Delbaere, L. J.; Roesler, W. J.; Falk, K. J.; Steer, R. P.; Lee, J. S. *J. Mol. Biol.* **1999**, *294*, 477–85.